Tooth Strength Study of Spur Planet Gears

Raymond J. Drago
Bapa R. Uppaluri
Boeing Vertol Company
Philadelphia, PA

Abstract

The finite-element method (FEM) has been applied to three spur planet gears to determine the tooth strength. Models for each gear were created using different constraint conditions and model parameters. Comparison of the results of the models with experimental data reveals the need to integrate the effect of the individual roller loads on the model. The effect of roller-bearing support on the gear tooth root and fillet stresses has been demonstrated to be a significant factor in gear load capacity.

The use and application of a system of updated finite-element pre- and postprocessors used in the analysis are briefly explained. One planet gear's static strain survey test data are presented and compared with both the FEM analytical predictions and conventional AGMA results. The usefulness of the FEM preprocessor and postprocessor in minimizing the test effort is pointed out.

Introduction

In the design of any new gear drive, the performance of previous similar designs is very carefully considered. In the course of evaluating one such new design, the authors were faced with the task of comparing it with two similar existing systems, both of which were operating quite successfully. A problem arose; however, when it was realized that the bending stress levels of the two baselines differed substantially. In order to investigate these differences and realistically compare them to the proposed new design, a three-dimensional finite-element method (FEM) approach was applied to all three gears. The general FEM methodology was similar to

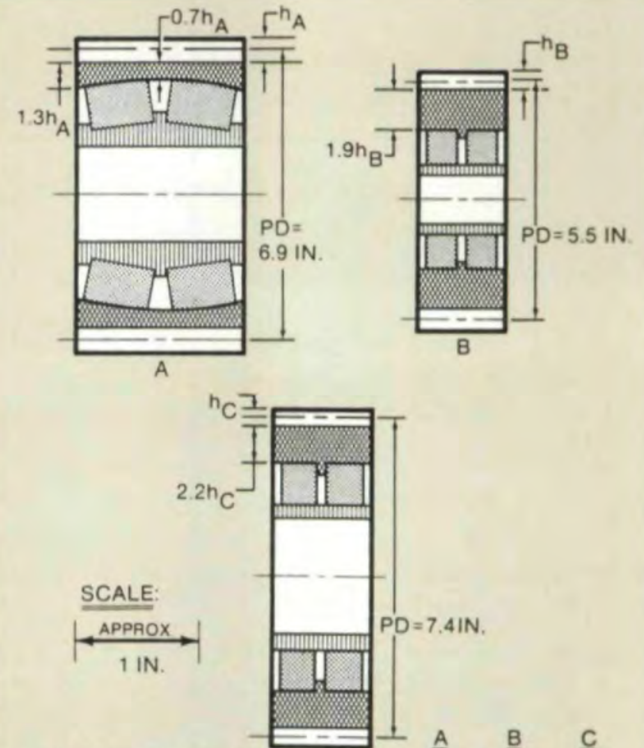

	A	B	C
DIAMETRAL PITCH (IN.)	4.8	7.8	5.8
AGMA BENDING STRESS (KSI)	37.0	66.2	41.4
HORSEPOWER/FACE WIDTH	187.5	206.0	353.3
TANGENTIAL LOAD/FACE WIDTH	3,418	3,712	3,544
MOMENT OF INERTIA OF RIM	0.06	0.04	0.12
HORSEPOWER/POUND (APPROX) (GEAR ONLY)	45	18	65

Fig. 1—Comparison of Three Planet Gears

that which the authors have applied extensively to spiral-bevel gears.[1-4] The basic accuracy of this system and its ability to accurately predict the stress levels of complex spiral-bevel gears has also been established.

Since all three systems are simple epicyclic drives, the planet gear of each was chosen for detailed evaluation. Although similar, as Fig. 1 shows, there are some substantial differences in the detailed construction and supporting structure for each.

Planet gears B and C are supported by double-row cylindrical roller bearings while planet gear A is supported by a double-row spherical bearing. The backup ratio (rim

AUTHORS:

MR. RAYMOND J. DRAGO *is a Senior Engineer with the Advanced Power Train Technology of Boeing's Vertol Company. Drago's current interests lie in the areas of applied mathematics, kinematics, analytical gear system design and synthesis, finite element analysis, and computer programming. He has also been pursuing ongoing studies in the analysis, design, manufacture, assembly, and testing of many gear systems. He holds a Bachelor of Mechanical Engineering Degree from the City University of New York and a Masters Degree in Structural Engineering from Pennsylvania State University.*

DR. BAPA UPPALURI *is a Senior Engineer in the Power Train Technology Department of Boeing Vertol Company. His areas of study focus on stress analysis, finite element methods using NASTRAN, ANSYS, WECAN, fatigue analysis, and computer programming. He earned a M.S.M.E. and a Ph.D. from Georgia Tech.*

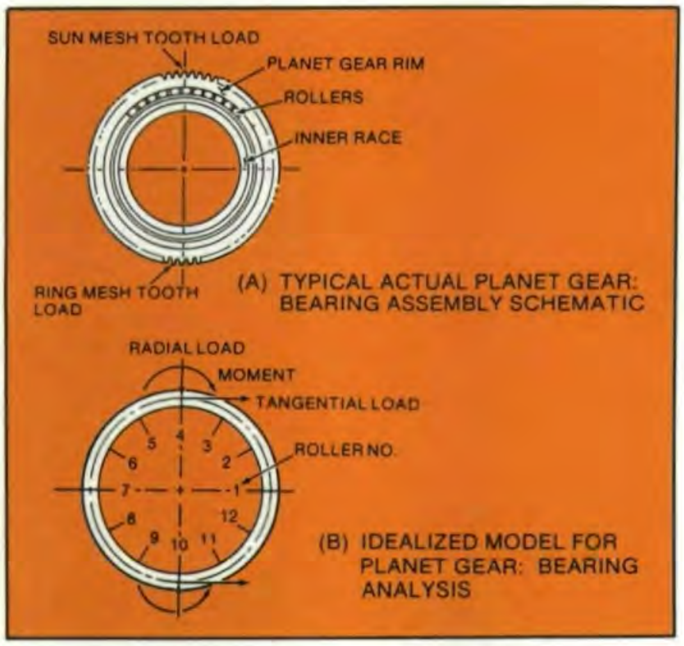

Fig. 2 – Planet Ring Program Analysis Model

thickness/whole depth), while similar for B and C, is quite different for A. The pitch diameters of planet gears A and C are similar while that for B is somewhat smaller.

Experience with other thin-rimmed gears has indicated that such gears must be modeled very carefully, in three dimensions, with all individual roller loads applied as constraint conditions.[6,7]

Method of Analysis

The method used was simple in concept, though rather complex in execution. The general procedure used for each gear was as follows:

1. **Reference Baseline** – Run each gear through AGMA-type gear analysis computer program in order to produce a common reference point.
2. **Define Roller Reaction Loads** – Analyze each planet gear/bearing system with computer program RINGEAR to define individual roller reaction loads and obtain inner- and outer-rim stress approximations.
3. **Preprocessing** – Model each gear using the FEM preprocessor.[3]
4. **NASTRAN FEM Analysis** – Load each model with appropriate sun mesh, ring mesh, and individual roller loads and execute NASTRAN analysis.
5. **Postprocessing** – Evaluate NASTRAN results using Boeing Vertol postprocessor and plot results.[3]

Once all of the data are available, they must be evaluated so that specific conclusions may be drawn.

In order to establish confidence in the comparative accuracy of this approach, the results of the planet gear A analysis were compared to the experimental data which were obtained from a strain survey. As will be obvious when the basic FEM tooth stresses are presented later, the correlation between test and FEM results is quite good.

Reference Baseline

Using general methodology[8] (but with all modifying factors set equal to unity), the AGMA tooth fillet bending stresses were calculated in order to provide a common frame of reference. These stresses, shown in Fig. 1, indicate that planet gear B is, by far, more highly stressed than either A or C. As the FEM analysis will show; however, this is not actually the case.

Define Roller Reaction Loads

In order to obtain an accurate estimate of the actual tooth root and fillet stresses, the FEM model must realistically simulate the actual structure being analyzed. Perhaps the single most common (and most devastating) error made in applying FEM to gearing is the failure to properly model the gear and its constraint conditions. In the case of the planet gears, the temptation to use a simply supported two-dimensional model is great. To do so, however, will yield apparently reasonable, but actually very misleading results.

Because of the dual function of the blank (gear teeth on the OD and bearing journal on the ID), the gear must be modeled not only with both sun and ring loads applied but

TABLE I. INPUT DATA FOR RIM STRESS AND DEFLECTION PROGRAM

First Card	Integer equal to number of cases being run
Second Card	Title for case
Third Card	Number of planets, pressure angle, helix angle, sun gear torque
Fourth Card	Ring gear pitch diameter, sun gear pitch diameter, planet gear pitch diameter, planet gear centroid diameter
Fifth Card	Ring gear centroid diameter, backup I and backup area, C distance to ID, C distance to OD
Sixth Card	Same information as above but for sun gear
Seventh Card	Same information as Card 5 but for ring gear at bolt holes
Eighth Card	I/C to planet gear root diameter, I/C to planet gear inside diameter, number of rollers per row, planet backup cross section area, planet backup moment of inertia
Ninth Card	Planet bearing effective roller length, diametral clearance, roller ID (hollow roller), inner race out of round
Tenth Card	Planet bearing roller diameter, bearing pitch diameter, bearing contact angle, planet speed relative to post

Preprocessing

The preprocessing step comprises two parts: tooth contact line definition and actual grid-by-grid FEM model definition.

Contact Line Analysis

The accurate application of gear tooth loads in the finite-element method required the coordinates of the contact lines from the beginning of mesh to the end. Computer programs have been developed to generate the contact lines for spur, helical, and bevel gear meshes based on the theory of conjugate action. The program generates contact lines on three adjacent teeth at regular angular position intervals from start to end of mesh. It also generates the unit inward normal vectors at the contact coordinates, which are subsequently used as the load vectors in the NASTRAN analysis.[3]

Table III illustrates the very simple input data required by the spur gear tooth contact line program.[2, 3]

Model Geometry Definition

The gear preprocessor computer program, developed by the authors, was used to create all three models used in this analysis.[2, 3] It generates a gear finite-element model built of solid CIHEX1 elements. As many teeth as needed can be molded, together with or without integral front and/or back shafting. It can automatically generate the executive, case control, and bulk data decks (with force cards) for COSMIC-NASTRAN linear static analysis. With a little manual editing of the data deck, in order to add boundary conditions (SPC/MPC/SPC1) or to combine loads if necessary, a complete NASTRAN analysis can be performed. Table IV presents the input data required for this preprocessor.

NASTRAN FEM Analysis

The data deck generated by the preprocessor requires some manual editing before being submitted for a NASTRAN analysis. The preprocessor employs a unit load distribution along the tooth contact lines to generate the NASTRAN force cards. The torque applied to the gear tooth due to this unit loading is calculated and provided as output. This unit loading torque must be multiplied by a load factor to obtain the actual torque transmitted by the gear. This is accomplished by means of the load cards in the NASTRAN data deck where linear combinations of forces are created. In addition, proper boundary conditions must be imposed on the model for the static analysis. The restraints must reflect the manner in which the gear is supported by its bearings; this is done by means of SPC or SPC1 or MPC cards in the NASTRAN program. Finally, the number of load cases to be run, the output data required from each load case, the plot options, etc, must be edited before submitting the NASTRAN job.

Each NASTRAN load case consists of many tooth load cases, each of which simulates the instantaneous contact loads at the sun/planet and planet/ring gear meshes. This allows the FEM model to simulate the response of the planet gear during a strain survey so that the data from both can be easily compared.

Postprocessing

The postprocessor reads the voluminous NASTRAN stress output file and generates stress tables and plots at the tooth fillet or root for each load case. The postprocessor interpolates the stress at adjacent grids to yield fillet and root stress distributions for all load cases individually and as a composite for a full mesh cycle. The resultant stresses are then summarized in the form of plots of maximum alternating and peak tension stress as functions of face width for both fillet and root locations for one complete gear revolution.[2, 3]

Results

The results of this analysis are best presented by comparing the stresses at three locations in the tooth fillet area, as defined in Fig. 4. The fillet location is the critical section implicit in the AGMA stress approach. The root location is often critical for thin-rimmed hollow gears, because, at the central root location, the tooth bending and ring bending stresses combine to yield high stress levels.

While the results of a purely analytical study are of interest, it is imperative that experimental verification of new methods be provided so that their validity can be evaluated. Fortunately, a substantial base of experimental data exists for one of the planet gears (A). These data, for both root and fillet locations, will be superimposed on the FEM results for comparative purposes.

Before the stress results are examined, however, some planet gear stiffness data are obtained from the ring analysis

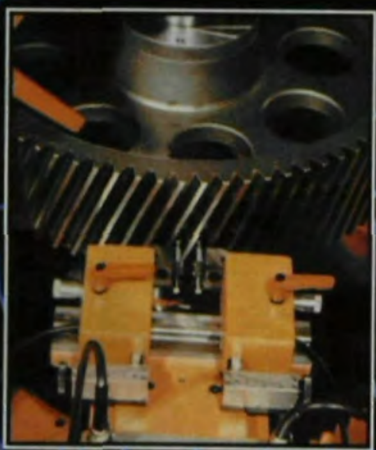


R INSPECTION
nd MACHINES

cking of gears and gear
of the manufacturing process.

StarCut now offers American manufacturers the full line of Hoefler Profile and Lead Measuring Machines, Pitch and Runout Inspection Equipment, and Double Flank Gear Rolling Testers.

Hoefler gear measuring equipment covers the full range from manually operated units to fully equipped measuring centers with computer controlled automatic measuring sequence. By interlinking controls of automatic inspection machines with the controls of flexible manufacturing cells an integration of gear inspection cycles is possible at different production stages of automatic gear manufacturing.

StarCut is now prepared to assist customers by furnishing gear inspection equipment and machines for any level of sophistication.

STARCUT SUPPLIED PRODUCTS AND SERVICES

Star Machine Tools
Standard and CNC Hob Sharpeners
Shaper Cutter Sharpeners
CNC Drill and Reamer Sharpeners

Star Cutting Tools
Hobs
Form-Relieved Cutters
Gun Drills
Gun Reamers
Keyseat Cutters

Gold Star Coatings

Lorenz
Shaper Cutters

Hurth Machine Tools
Automatic Spline Shaft Milling Machines
CNC Gear Shaving Machines
CNC Gear Rolling Machines
Gear Testing Machines
Shaving Cutter Grinding Machines
CNC Gear Tooth Chamfering Machines
Gear Deburring Machines
CNC Hard Gear Finishing Machines

Hoefler
CNC Inspection Equipment for Gears and Gear Cutting Tools

TiN Coating Systems
Complete Turnkey Applications

PLANRING
Planning & Engineering
Flexible Machining Systems

Stieber
Precision Clamping Tools

Please contact us for detailed information on this complete Hoefler line of gear inspection equipment and machines.

Visit Us at Booth 6343
IMTS
1986 INTERNATIONAL MACHINE TOOL SHOW

Since 1927
Star
STARCUT SALES, INC.
23461 Industrial Park Drive
Farmington Hills, MI 48024
313/474-8200 Telex 230-411

CIRCLE A-5 ON READER REPLY CARD

TABLE IV. SPUR AND HELICAL GEAR GEOMETRIC PREPROCESSOR INPUT DATA

Card No.	Item	Format/Location
1	A. Title	Alphanumeric-1-80
2	A. Letters "ELEM"	Real, 1-4
	B. No. of teeth in gear	Real, 5-14
	C. No. of full teeth modeled	Real, 15-24
	D. No. of layers of elements along face	Real, 25-34
	E. No. of rows of elements in half tooth	Real, 35-44
	F. No. of rows of elements in half blank	Real, 45-54
3	A. Letters "FULL"	Real, 1-4
	B. Location no. of full tooth	Real, 5-14
	C. Location no. of full tooth	Real, 15-24
	D. Location no. of full tooth	Real, 25-34
	E. Location no. of full tooth	Real, 35-44
	F. Location no. of full tooth	Real, 45-54
	G. Location no. of full tooth	Real, 55-64
	(Repeat Card 3 if more than six full teeth are generated)	
4	A. Letters "PROF"	Real, 1-4
	B. Tooth blank factor (≈ 0.95)	Real, 5-14
	C. Kink factor (≈ 0.95)	Real, 15-24
	D. No. of grids on profile	Real, 25-34
	E. No. of grids on centerline of tooth	Real, 35-44
5	A. Letters "PROF"	Real, 1-4
	B. Line no. of profile grid no. 1	Real, 5-14
	C. Line no. of profile grid no. 2	Real, 15-24
	D. Line no. of profile grid no. 3	Real, 25-34
	E. Line no. of profile grid no. 4	Real, 35-44
	F. Line no. of profile grid no. 5	Real, 45-54
	G. Line no. of profile grid no. 6	Real, 55-64
	(Repeat Card 5 if needed; lines 1 and 58 should be included)	
6	A. Letters "LODL" for loading left face of tooth	Real, 1-4
	B. Tooth no. is FEM model to be loading	Real, 5-14
	C. Tooth no. is contact program generating contact line	Real, 15-24
	D. Mesh position no. is contact program generating contact line	Real, 25-34
7	A. Letters "SPUR"	Real, 1-4
	B. Gear inner radius	Real, 5-14
	C. Gear outer radius	Real, 15-24
	D. Gear base radius	Real, 25-34
	E. Gear pitch radius	Real, 35-44
	F. Gear fillet radius	Real, 45-54
	G. Gear Fillet tangency radius	Real, 55-64
8	A. Letters "SPUR"	Real, 1-4
	B. No. of teeth	Real, 5-14
	C. Face width, in.	Real, 15-24
	D. Helix angle, degrees +LH, −RH	Real, 25-34
	E. Pressure angle, degrees	Real, 35-44
	F. Arc tooth thickness, in.	Real, 45-54

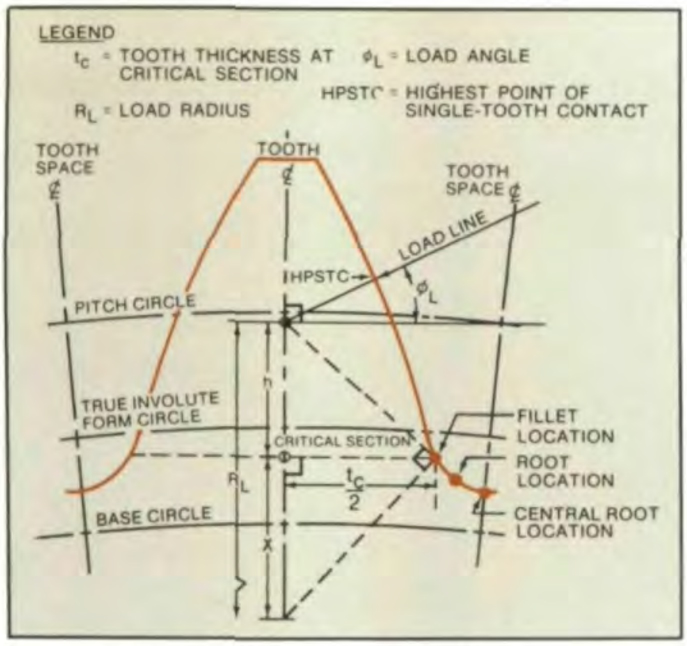

Fig. 4—Tooth Form Stress Layout Schematic

and used to define the roller loads.

Ring Deflections

The stress results from the ring analysis have already been presented. As noted, they are of comparative interest only because they do not reflect the stress concentrations caused by the tooth roots. The ring program also provides the radial ring deflection at each roller location. This information is used to define the reaction loads. Additionally, however, it can provide some insight into the rigidity of the gears. As Table V shows, these deflections are far from insignificant in aircraft transmissions.

The need to include this effect in the overall analysis of the planet gear stresses should be understood.

Fillet Stresses

Fig. 5 shows the fillet stress results for all three planet gears with the experimental results for planet gear A also superimposed on that plot. Since muliple strain gages were applied to muliple teeth, both the range of measured data and the mean are shown. The calculated and measured values for planet gear A are in very close agreement.

If the analysis is similarly accurate for planet gears B and C, the fillet stresses for all three gears are much closer than the simple AGMA results would indicate. In fact, although the AGMA stresses for planet gear B are much higher than for A, the FEM analysis indicates that the alternating stresses for both gears are about equal. Interestingly, the fillet alternating stress level for planet gear C is actually lower than that for either A or B.

Root Stresses

Very similar results were obtained at the root location (Fig. 6). The correlation between test an analysis was again quite good, especially for the alternating stresses. As was the case with the fillet stresses, the maximum alternating root stresses on planet gears A and B are quite close. However, the peak stress level on planet gear B is significantly higher than that on planet gear A, while that on planet gear C is higher than either A or B. The alternating stress on planet gear C is actually lower than that for either of the other planets.

Central Root Stresses

The tooth fillet and root stresses described above are useful in evaluating the capacity of the gear teeth as influenced by many factors, including the behavior of the ring that supports the teeth. Due to the complex loading applied to this ring, the basic ring stresses are also of interest. (The authors

TABLE V. RADIAL RIM DEFLECTIONS AT ROLLERS

Roller No.*	Radial Deflection (in.)		
	Planet A	Planet B	Planet C
1	0.0025	0.0024	0.0022
2, 14	0.0028	0.0026	0.0023
3, 13	0.0030	0.0028	0.0025
4, 12	0.0031	0.0027	0.0025
5, 11	0.0023	0.0016	0.0015
6, 10	−0.0019	−0.0019	−0.0017
7, 9	−0.0065	−0.0055	−0.0050
8	−0.0083	−0.0070	−0.0064

*See Figure 2 for roller numbering scheme.

have investigated at least one planet gear failure which was traced to excessive central root stresses). The RINGEAR program approximates these stresses through the idealization shown in Fig. 3. However, the effect of the tooth fillets (which are stress risers on the ring OD) is not included. By looking at the FEM results for a central root location, a more accurate picture of these ring stresses (Fig. 7) can be obtained. Comparing these charts with those shown in Fig. 3 shows the effect of the tooth loading and the tooth fillets. The effect of the thinner planet gear A ring on the stress distribution as compared to the stiffer planet gear C ring is also apparent.

The maximum tension and compression peaks for most gears are associated with the tooth mesh itself. From Fig. 7, however, it can easily be seen that the compressive stress due to the ring bending, independent of the mesh contact, exceeds that due to the tooth mesh itself. The alternating stress at this location is thus defined by combining the peak tension due to the tooth mesh with the peak compressive stress due to the ring bending. This is a critical consideration and can be the governing factor in defining the load capacity of thin-rimmed, roller-supported planets.

Summary

Although the basic AGMA tooth fillet stresses for the three planets evaluated here differ substantially, their fatigue (alternating) stress levels are surprisingly similar, as the summary in Table VI shows.

The conventional AGMA tooth bending stresses are closer to the FEM peak tension stresses (Table VI) at the fillet location than at the root location. This may be attributed to the fact that the effect of rollers is more predominant at the tooth root than at the tooth fillet. The roller effect is not considered in AGMA calculation.

Discussion

The correlation between the static-strain survey test data and the FEM results for planet gear A is in general about 15 percent. Considering the possible test variations to be about 10 percent by themselves, this level of correlation appears to be quite acceptable.

The effect of rollers on the tooth stresses appears to be a function of the backup rim's rigidity and tooth loads. Planet gear C has the largest backup rim moment of inertia and produces a tensile steady stress (Table VI) at all locations considered. Planet gear A has half the backup rim rigidity and twice the tooth load. The FEM analysis predicted compressive steady stresses at tooth root and fillet locations as verified by test data.

Although in all three cases considered here, the critical stress location is not at the central root location, the possibility of this location's becoming critical is certainly obvious. A small additional stress concentration, for example, would tip the scales. Generally, in the absence of integral roller bearings, maximum tooth stresses occur during the mesh. Futhermore, the magnitude of the peak stresses with rollers could be higher than those without rollers. As pointed out earlier, this effect is a function of the rigidity of backup rim and tooth load.

An interesting observation, or more correctly, conjecture,

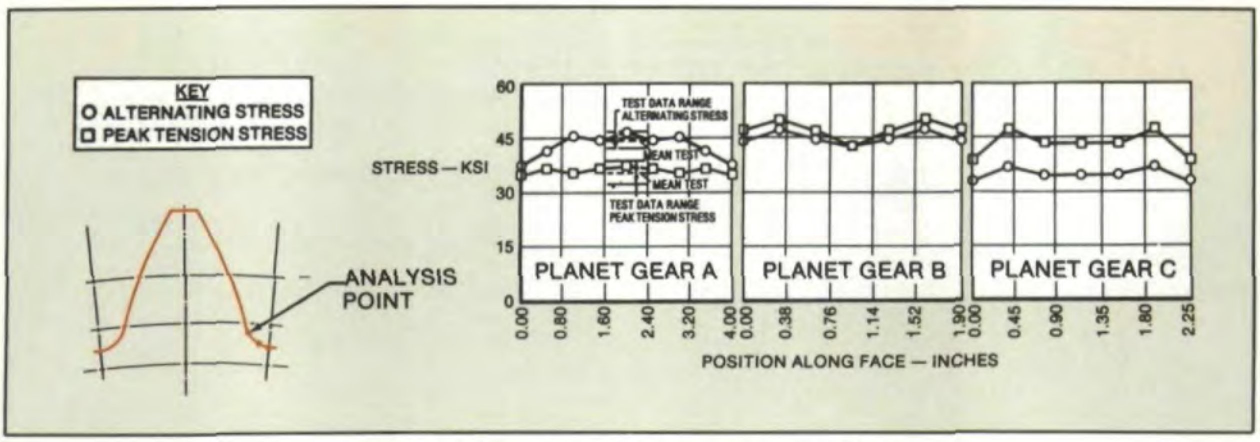

Fig. 5 – FEM Gear Tooth Fillet Stresses Versus Face Width

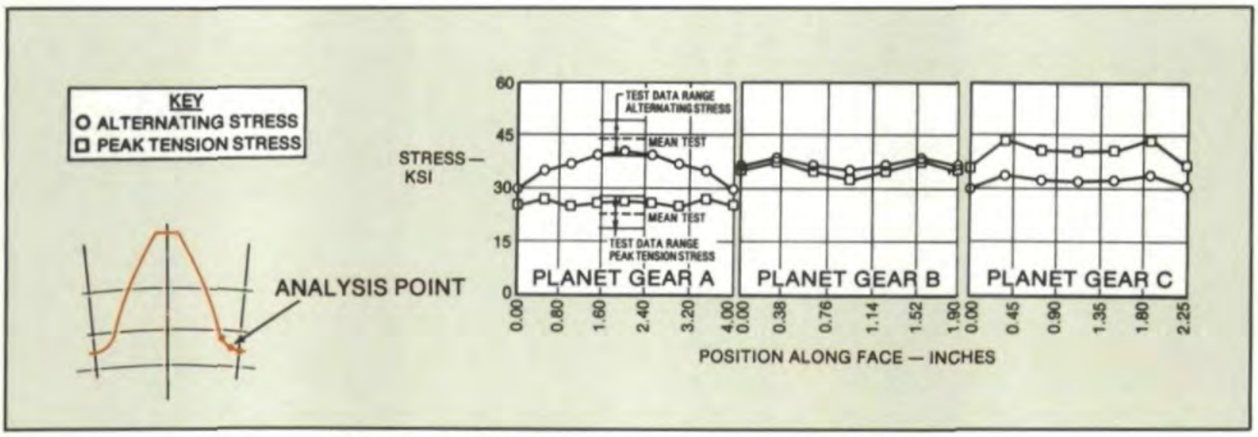

Fig. 6 – FEM Gear Tooth Root Stresses Versus Face Width

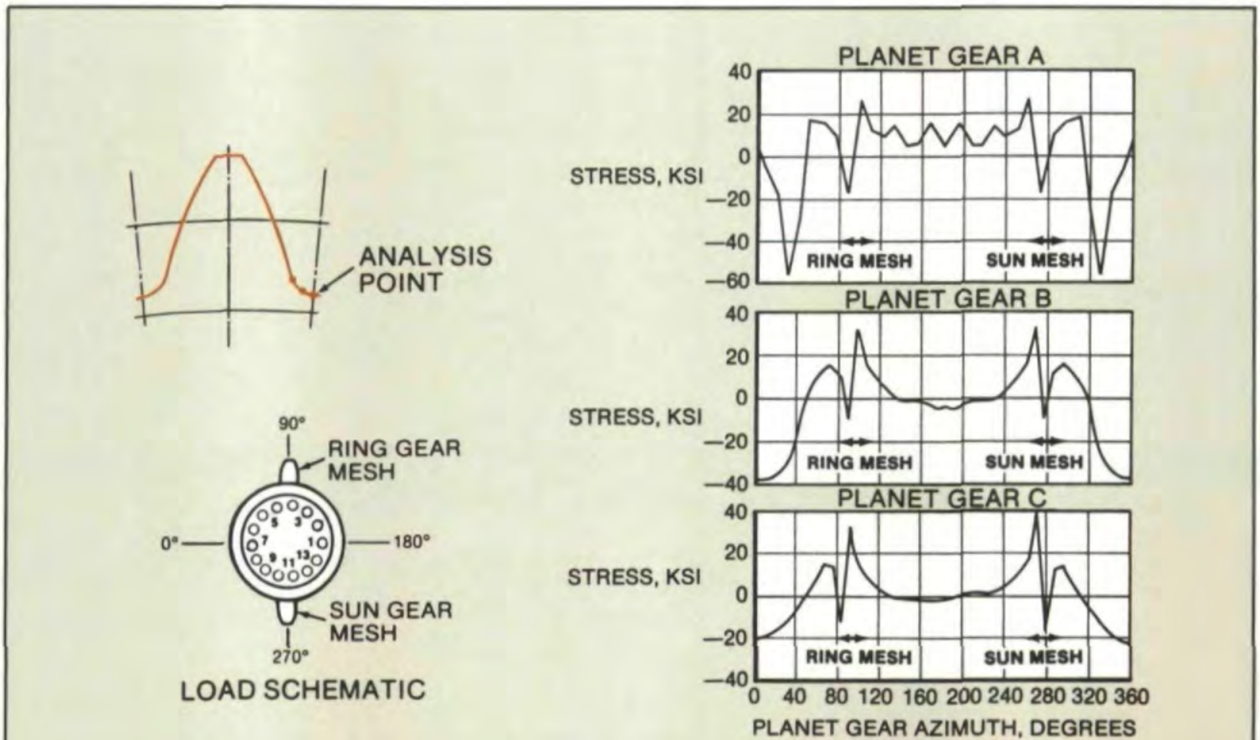

Fig. 7 – FEM Central Root Stresses

TABLE VI. SUMMARY OF PREDICTED STRESSES

Stress Item	Planet A (ksi)	Planet B (ksi)	Planet C (ksi)
AGMA *Tooth bending at sun mesh*[1]	*37.0*	*66.2*	*41.4*
FEM peak tension at tooth fillet[2]	38.1	50.8	40.4
FEM fatigue stress at tooth fillet[2,3]	-9.7 ± 47.8	$+2.8 \pm 48.0$	$+10.6 \pm 37.2$
FEM fatigue stress at tooth root[2,3]	-14.2 ± 40.9	-1.1 ± 38.7	$+9.8 \pm 33.0$
FEM fatigue stress at central root[2,3]	-14.2 ± 41.8	-4.5 ± 35.3	$+16.5 \pm 31.3$

NOTES: 1. Does not consider effect of roller loads
2. Includes effect of bearing roller loads
3. Considers both sum mesh and ring mesh

comes to mind based on these data. In some designs, the planet gear is supported by an integral, fluid-film bearing. Since such a bearing provides a fully distributed load reaction rather than discrete individual (roller) reaction loads, it is possible that such planet gears may be designed with thinner rims than their roller-bearing-supported counterparts. This possibility has not been investigated so far and could be undertaken in the future.

The AGMA and FEM calculated peak tension stresses for planet gears A and C agree rather well; those for planet gear B do not. A possible explanation for this is the AGMA stress correction factor. The smaller fillet radii on finer pitch gears tend to produce comparatively large values for the stress correction factor. These values may be somewhat pessimistic for finer pitch gears. The empirical relation used to calculate this factor is based on work by Dolan and Broughamer which used relatively large models; thus the extrapolation to small fillets may be in error.

Conclusions

After carefully studying all the data, the following specific conclusions were reached:

1. Despite the apparent large differences in the AGMA stress levels for the three planet gears, their alternating stresses are quite similar.
2. The FEM analysis described, using the gear preprocessor and postprocessor, is a reliable tool for analyzing spur planetary gears with integral roller bearings.
3. In critical applications which typically involve extensive testing (strain surveys), the FEM analysis could be substituted for selected test conditions after establishing correlation with some known test conditions, thereby reducing test time, cost, and effort.
4. The effect of the ring bending-induced compressive stress on the alternating stress in the tooth root is not negligible and may be the governing factor in some circumstances.

Recommendations

Thus far, the gear finite-element model generated by the preprocessor is used successfully in predicting the tooth stresses for spur and spiral-bevel gears by a linear static analysis. The potential which exists for extending this methodology is substantial. Consider the following examples:

1. The same FEM model could probably be used in a dynamic analysis to predict the gear natural frequencies and normal mode shapes.
2. A nonlinear, static, FEM analysis, wherein the tooth contact loads are a function of the tooth deflections, could shed more light on tooth load distribution along the contact lines and tooth load sharing among adjacent gear teeth.
3. A comprehensive program of parametric study of spur, helical, and bevel-gear tooth stresses with respect to diametral pitch, backup rigidity, contact pattern, and load distribution might be undertaken with the ultimate goal of arriving at optimally minimum-weight aircraft

transmission gears.

4. The effect of the thermal deformation of transmission housings, particularly lightweight magnesium, aluminum, or composite housings such as those usually used in aerospace applications, is to cause gear misalignment. This shifts the contact pattern on the gear tooth and causes higher tooth stresses than in the case of perfectly aligned gears, and might lead to premature fatigue failure. The use of the FEM analysis for a better understanding of this problem and its solution should be considered.
5. The expression used for the stress-correction factor in the AGMA method should be reviewed for applicability to small fillets.

References

1. DRAGO, RAYMOND J., On The Automatic Generation of FEM Models for Complex Gears – A Work-In-Progress Report, American Gear Manufacturers Association Aerospace Gearing Meeting, San Diego, CA, February 1982.
2. DRAGO, RAYMOND J., and UPPALURI, BAPA R., Large Rotorcraft Transmission Technology Development Program, Vol. 1, NASA Report CR-168116, National Aeronautics and Space Administration, Cleveland, OH, February 1983.
3. DRAGO, RAYMOND J., and UPPALURI, BAPA R., Computer Program Users Manual, Vol. II, Large Rotorcraft Transmission Technology Development Program, NASA Report CR-168117, National Aeronautics and Space Administration, Cleveland, OH, February 1983.
4. DRAGO, RAYMOND J., SAMANICH, N.E. and MACK, J.C., Development of Large Rotorcraft Transmissions, American Helicopter Society, Thirty-Ninth Annual Forum, St. Louis, MO, May 1983.
5. DRAGO, RAYMOND J., Results of an Experimental Program Utilized to Verify a New Gear Tooth Strength Analysis, American Gear Manufacturers Association, Fall Technical Meeting, Montreal, Canada, October 1983.
6. DRAGO, RAYMOND J., and PIZZIGATI, G.A., Some Progress in the Accurate Evaluation of Tooth Root and Fillet Stresses in Light Weight, Thin Rimmed Gears, AGMA Paper No. 229.21, American Gear Manufacturers Association Fall Technical Meeting, Washington, DC, October 1980.
7. DRAGO, RAYMOND J., BROWN, F.W., and FAUST, H.S., Recent Advances in the Evaluation of Stresses in High Speed, Light Weight, Highly Loaded Gearing, International Conference on Reliability, Stress Analysis, and Failure Prevention, San Francisco, CA, August 1980.
8. AGMA Standard for Rating the Pitting Resistance and Bending Strength of Spur and Helical Involute Gear Teeth, AGMA 218, American Gear Manufacturers Association, Arlington, VA.
9. JONES, A.B., and HARRIS, T.A., Analysis of a Rolling Element Idler Gear Bearing Having a Deformable Outer-Race Structure, Journal of Basic Engineering, June 1983.

This article was previously presented at the AGMA Fall Technical Meeting in October 1984. Paper No. 84FTM1.